

# Distributed Routing Algorithms for Underwater Acoustic Sensor Networks

Dario Pompili, *Member, IEEE*, Tommaso Melodia, *Member, IEEE*, and Ian F. Akyildiz, *Fellow, IEEE*

**Abstract**—Underwater Acoustic Sensor Networks (UW-ASNs) consist of devices with sensing, processing, and communication capabilities that are deployed underwater to perform collaborative monitoring tasks to support a broad range of applications. The enabling communication technology for distances over one hundred meters is wireless acoustic networking because of the high attenuation and scattering affecting radio and optical waves, respectively. In this work, the problem of data gathering is investigated by considering the interactions between the routing functions and the characteristics of the underwater acoustic channel. Two distributed geographical routing algorithms for delay-insensitive and delay-sensitive applications are proposed and shown through simulation experiments to meet the application requirements.

**Index Terms**—Underwater wireless communications, underwater sensor networks, routing algorithms, optimization.

## I. INTRODUCTION

UNDERWATER Acoustic Sensor Networks (UW-ASNs) [1], [2] consist of devices with sensing, processing, and communication capabilities that are deployed to perform collaborative monitoring tasks in a given body of water. UW-ASNs are envisioned to support applications for oceanographic data collection, ocean sampling, pollution and environmental monitoring, offshore exploration, disaster prevention, assisted navigation, distributed tactical surveillance, and mine reconnaissance. To make underwater applications viable, there is a need to enable efficient communication protocols among underwater devices, which are based on acoustic wireless technology for distances over one hundred meters because of the high attenuation and scattering affecting radio and optical waves, respectively.

Although there exist many network protocols for terrestrial wireless sensor networks, the unique characteristics of the underwater acoustic communication channel, such as limited bandwidth capacity [3] and high propagation delays [4], require new efficient and reliable data communication protocols. Major challenges in the design of UW-ASNs are: i) the propagation delay is five orders of magnitude higher than in

radio frequency (RF) terrestrial channels, which is due to the low speed of sound (1500 m/s) [5]; ii) the underwater acoustic channel is severely impaired, especially due to multipath and fading problems; iii) the available bandwidth is distance dependent and in general is limited to few tens of kHz due to high environmental noise at low frequencies (lower than 1 kHz) and high transmission loss at high frequencies (greater than 50 kHz) [6], [7]; iv) high bit error rates and temporary losses of connectivity can lead to the formation of ‘shadow zones’, underwater regions where the signal reception is impaired due to deep signal dips and fading caused by multipath [8]; v) underwater sensors are prone to failures because of fouling and corrosion; vi) batteries are energy constrained and cannot be recharged (solar energy cannot be exploited underwater).

In this article, we propose two bandwidth- and energy-efficient distributed geographical routing algorithms that are designed to meet the requirements of delay-insensitive and delay-sensitive static underwater sensor network applications. The proposed routing solutions are tailored for the characteristics of the 3D underwater environment, e.g., they take into account the very high propagation delay, which may vary in horizontal and vertical links, the different components of the transmission loss, the impairment of the physical channel, the limited bandwidth, and the high bit error rate. These characteristics lead to a very low utilization of the underwater acoustic channel when communication protocols not specifically designed for this environment are adopted.

Our routing solutions allow achieving two conflicting objectives, i.e., 1) increasing the efficiency of the acoustic channel and 2) limiting the packet error rate on each link. In other words, this conflict is between achieving high channel efficiency (which requires longer packets) and maintaining low packet error rate (which requires smaller packets). This problem is resolved by letting a sender transmit a *train* of short packets *back-to-back* without releasing the channel. Specifically, the proposed routing algorithms allow each node to *jointly* select its best next hop, the optimal transmit power, and the forward error correction (FEC) rate for each packet, with the objective of minimizing the energy consumption, while taking the condition of the underwater channel and the application requirements into account. Note that, while the proposed solutions are tailored for static networks and do not account for mobility issues, their distributed nature helps in case of mobility. While the optimal packet size is set *off-line* (whose choice is motivated by the need for system simplicity and ease of sensor buffer management, as described in [2]), the distributed algorithms adjust *on-line* the strength of the

Manuscript received February 2, 2010; revised May 3, 2010; accepted June 21, 2010. The associate editor coordinating the review of this paper and approving it for publication was I. Habib.

D. Pompili is with the Department of Electrical and Computer Engineering, Rutgers University, 94 Brett Road, Piscataway, NJ 08854 (e-mail: pompili@ece.rutgers.edu).

T. Melodia is with the Department of Electrical Engineering, University at Buffalo, The State University of New York, 332 Bonner Hall, Buffalo, NY 14260 (e-mail: tmelodia@eng.buffalo.edu).

I. F. Akyildiz is the director of the Broadband Wireless Networking Laboratory, School of Electrical and Computer Engineering, Georgia Institute of Technology, 75 5th Street, Atlanta, GA 30332 (e-mail: ian@ece.gatech.edu).

Digital Object Identifier 10.1109/TWC.2010.070910.100145

FEC technique when channel coding is performed by tuning the amount of FEC redundancy according to the dynamic channel conditions. Hence, given the off-line optimized fixed packet size, when the amount of FEC redundancy increases, the packet payload used for data decreases.

The remainder of this article is organized as follows. In Sect. II, we discuss the suitability of existing ad hoc and sensor routing solutions for the underwater environment, and motivate the use of geographical routing for UW-ASNs. In Sect. III, we present the 3D communication architecture considered, and we introduce the network and propagation models. In Sect. IV, we propose the packet-train concept to improve the underwater acoustic channel efficiency. In Sect. V, we introduce a distributed routing algorithm for delay-insensitive applications, while in Sect. VI we adapt it to statistically meet the end-to-end delay-sensitive application requirements. Finally, in Sect. VII, we show the performance results of the proposed solutions, and in Sect. VIII we draw the main conclusions.

## II. RELATED WORK

There has been an intensive study in routing protocols for terrestrial wireless ad hoc [9] and sensor networks [10] in the last few years. Because of the unique characteristics of the propagation of acoustic waves in the underwater environment, however, there are several drawbacks with respect to the suitability of existing terrestrial routing solutions for underwater networks. Routing protocols are usually divided into three categories, namely *proactive*, *reactive*, and *geographical* routing protocols.

*Proactive protocols* (e.g., DSDV, OLSR) provoke a large signaling overhead to establish routes for the first time and each time the network topology is modified because of mobility, node failures, or channel state changes, as updated topology information has to be propagated to all network devices. In this way, each device is able to establish a path to any other node in the network, which may not be needed in UW-ASNs. Also, scalability is a critical issue for this family of routing schemes. For these reasons, proactive protocols are not suitable for underwater sensor networks.

*Reactive protocols* (e.g., AODV, DSR) are more appropriate for dynamic environments but incur a higher latency and still require source-initiated flooding of control packets to establish paths. Reactive protocols are unsuitable for UW-ASNs as they also cause a high latency in the establishment of paths, which is even amplified underwater by the slow propagation of acoustic signals. Moreover, the topology of static UW-ASNs is unlikely to vary much on a short-time scale.

*Geographical protocols* (e.g., GFG, PTKF [11]) are very promising for their scalability feature and limited required signaling. However, Global Positioning System (GPS) radio receivers, which may be used in terrestrial systems to accurately estimate the geographical location of sensor nodes, do not work properly in the underwater environment. In fact, GPS uses waves in the 1.5 GHz and those waves do not propagate in water. Still, underwater sensing devices need to estimate their current position, irrespective of the chosen routing approach. In fact, as in most sensor networks, it is

necessary to associate the sampled data with the 3D position of the device that generates the data in order to spatially reconstruct the characteristics of the event at the surface station (sink). Underwater localization can be achieved by exploiting the low speed of sound in water, which permits accurate measurements of distances traveled by signals. The reader interested in the challenges to enable underwater localization is referred to [12], which provides a survey discussing and comparing several localization algorithms tailored for UW-ASNs.

Some recent work proposed network-layer protocols specifically designed for underwater acoustic networks. In [13], a routing protocol is proposed that autonomously establishes the underwater network topology, controls network resources, and establishes network flows, which relies on a centralized network manager running on a surface station. Although the idea is promising, the performance of the proposed mechanisms has not been thoroughly studied. In [14], the problem of data gathering for three-dimensional underwater sensor networks tailored for long-term monitoring missions is investigated, with a particular emphasis to resiliency; while the provided routing solution is optimal, little reconfiguration is allowed in case of node mobility or channel state changes. In [15], a vector-based forwarding routing is developed, which does not require state information on the sensors and only involves a small fraction of the nodes. The algorithm, however, does not consider applications with different requirements. In [16], the authors investigate the delay-reliability trade-off for multi-hop underwater acoustic networks, and compare multi-hop versus single-hop routing strategies while considering the overall throughput. The analysis shows that increasing the number of hops improves both the achievable information rate and reliability. In [17], the authors provide a simple design example of a shallow water network where routes are established by a central manager based on neighborhood information gathered from all nodes by means of poll packets. However, the authors do not describe routing issues in detail, nor do they discuss the criteria used to select data paths. Moreover, sensors are only deployed linearly along a stretch, and the characteristics of the 3D underwater environment are not investigated. In [18], a long-term monitoring platform for underwater sensor networks consisting of static and mobile nodes is proposed, and hardware and software architectures are described. The nodes communicate point-to-point using a high-speed optical communication system and broadcast using an acoustic protocol. The mobile nodes, called mules, can locate and hover above the static nodes for data muling, and can perform useful network maintenance functions such as deployment, relocation, and recovery. However, due to the limitations of optical transmissions, communication is enabled only when the sensors and the mobile mules are in close proximity. In [19], three versions of a reliable unicast protocol are proposed, which integrate Medium Access Control (MAC) and routing functionalities and exploit different levels of neighbor knowledge: (i) no neighbor knowledge, (ii) one-hop neighbor knowledge, and (iii) two-hop neighbor knowledge. The protocols, which rely on controlled broadcasting with no power control, have been compared in static as well as mobile scenarios in terms of different end-to-end networking metrics

(packet delivery ratio, packet delay, and energy consumption), leading to the following conclusions: 1) The three versions of the protocol outperform solutions that do not fully exploit neighbor knowledge in the design phase; 2) In a static environment, no version is optimal for all the metrics considered; 3) The higher the mobility, the lower the amount of information needed for making good routing decisions.

### III. ARCHITECTURE AND NETWORK MODELS

In this section, we consider a communication architecture for three-dimensional underwater sensor networks, and the network and propagation models that will be used in the formulation of our routing algorithms. Three-dimensional networks can perform cooperative sampling of the 3D ocean environment, and are used to detect and observe phenomena that cannot be adequately observed by means of ocean bottom sensor nodes. In fact, in three-dimensional underwater networks, underwater sensor nodes float at different depths to observe a given phenomenon. While the study of deployment strategies for 3D UW-ASNs are out of the scope of this work, the reader interested in deployment issues for such networks is referred to [20].

The underwater network can be represented as a directional graph  $\mathcal{G}(\mathcal{V}, \mathcal{E})$ , where  $\mathcal{V} = \{v_1, \dots, v_N\}$  is a set of nodes in a 3D volume, with  $N = |\mathcal{V}|$ , and  $\mathcal{E}$  is the set of directional links among nodes;  $e_{ij} \in \mathcal{E}$  equals 1 if node  $v_j$  is in the neighborhood of node  $v_i$ , i.e., if  $v_j$  can successfully decode packets transmitted by  $v_i$ . Note that,  $e_{ij}$  and  $e_{ji}$  may not have the same value as underwater links may be asymmetric. Node  $v_N$  (also  $N$  for simplicity) represents the sink, i.e., the surface station. Each link  $e_{ij}$  is associated with its distance  $d_{ij}$  [m], expected propagation delay  $T_{ij}^q = d_{ij}/q_{ij}$  [s], where  $q_{ij}$  [m/s] is the acoustic propagation speed of link  $(i, j)$ , and with the standard deviation of the propagation delay,  $\sigma_{ij}^q$  [s]. In [21], the underwater acoustic propagation speed  $q(z, s, t)$  [m/s] is modeled as,

$$q(z, s, t) = 1449.05 + 45.7 \cdot t - 5.21 \cdot t^2 + 0.23 \cdot t^3 + \\ + (1.333 - 0.126 \cdot t + 0.009 \cdot t^2) \cdot (s - 35) + \\ + 16.3 \cdot z + 0.18 \cdot z^2, \quad (1)$$

where  $t = T/10$  ( $T$  is the temperature in  $^{\circ}\text{C}$ ),  $s$  is the salinity in ppt, and  $z$  is the depth in km. The above expression provides a useful tool to determine the propagation speed in different operating conditions, and yields values in [1460, 1520] m/s. All these values, i.e.,  $e_{ij}$ ,  $T_{ij}^q$ , and  $\sigma_{ij}^q$ , are dependent on the 3D positions of nodes  $v_i$  and  $v_j$  (also  $i$  and  $j$  for simplicity in the following). Finally,  $\mathcal{S}$  is the set of sources, which includes those sensors that sense information and send it to the surface station,  $N$ .

The underwater transmission loss describes how the acoustic intensity decreases as an acoustic pressure wave propagates outwards from a sound source. The transmission loss  $TL(d, f)$  [dB] that a narrow-band acoustic signal centered at frequency  $f$  [kHz] experiences along a distance  $d$  [m] can be described by the Urick propagation model [21],  $TL(d, f) = \chi \cdot 10 \text{Log}(d) + \alpha(f) \cdot d + A$ . The first term accounts for the *geometric spreading*, which refers to the spreading of sound energy as a result of the expansion of the wavefronts.

It increases with the propagation distance and is independent of frequency. There are two kinds of geometric spreading: *spherical* (omni-directional point source, spreading coefficient  $\chi = 2$ ), which characterizes deep water communications, and *cylindrical* (horizontal radiation only, spreading coefficient  $\chi = 1$ ), which characterizes shallow water communications; note that in oceanographic literature *deep water* refers to water deeper than 100 m, whereas *shallow water* is shallower than that. In-between cases show a spreading coefficient  $\chi$  in the interval  $(1, 2)$ , depending on water depth and link length. The second term accounts for the *medium absorption*, where  $\alpha(f)$  [dB/m] represents an absorption coefficient that describes the dependency of the transmission loss on the central frequency. Finally, the last term, expressed by the quantity  $A$  [dB], is the so-called *transmission anomaly* and roughly accounts for the degradation of the acoustic intensity caused by multiple path propagation, refraction, diffraction, and scattering of sound caused by particulates, bubbles, and plankton within the water column. Its value is higher for shallow-water horizontal links (up to 10 dB), which are more affected by multipath [21].

### IV. CHANNEL EFFICIENCY AND PACKET TRAIN

In this section, we study the effect of the characteristics of the underwater environment on the *acoustic channel utilization efficiency*, which is defined as *the net bit rate achievable on a link when considering packet retransmissions due to channel impairments*, and provide guidelines for the design of routing solutions. When a random access technique is adopted to transmit a data packet in the shared acoustic medium (which is a common MAC protocol used by the underwater acoustic modems developed by WHOI and Benthos), a trade-off between channel efficiency and link reliability occurs - in fact, while the former increases the latter decreases with the increase of the packet size. Conversely, our routing solutions allow achieving two conflicting objectives, i.e., increasing the efficiency of the acoustic channel by transmitting a *train* of short packets *back-to-back*; and limiting the packet error rate by keeping the length of the transmitted packets short.

In the following, we propose the *packet-train* scheme to enhance the channel efficiency and summarize the design philosophy to set the optimal packet size, whose optimization problem is mathematically cast in [2]. While the optimal packet size at the data link layer in an underwater channel has been analytically derived in [22], our analysis in [2] accounts for cross-layer interactions with MAC and forward error correction (FEC) schemes. The packet optimization analysis in [22], in fact, does not consider the additional overhead caused by the adopted FEC scheme, nor does it evaluate the number of required packet retransmissions, which depends on the experienced packet error rate (PER).

In [2], we considered a shared channel where a device adopts a *single-packet* transmission scheme, i.e., transmits a data packet when it senses the channel idle, and the corresponding device advertises a correct reception with a short acknowledgement (ACK) packet. The payload of the data packet to be transmitted is assumed to have size  $L_P^D$  bits, while the header  $L_P^H$  bits. Moreover, the packet may be protected with a FEC mechanism, which introduces a redundancy of  $L_P^E$  bits. Note that in the notation used in the following to

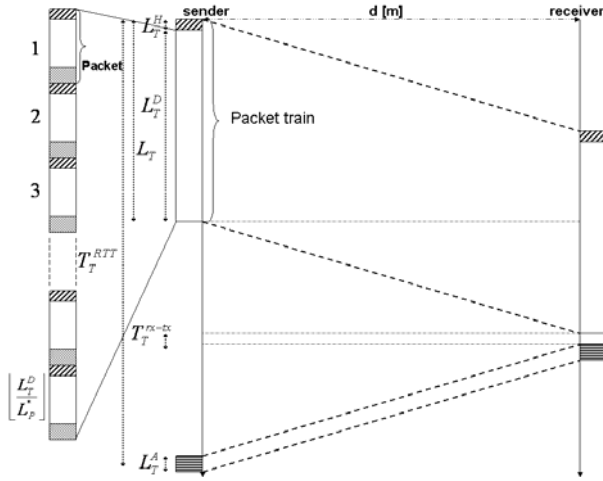


Fig. 1. Packet-train transmission scheme.

represent variables and parameters, the subscripts  $P$  and  $T$  are associated with packets and trains, respectively. A thorough analysis of the performance of the single-packet transmission scheme in underwater channels can be found in [2]. Here, we summarize the findings and provide some observations:

- 1) *The channel utilization efficiency is very low.* This, combined with very low shared data rates in the order of tens of kbps, may be detrimental for communications. Hence, it is crucial to maximize the efficiency in exploiting the limited available bandwidth.
- 2) *Underwater communications greatly benefit from the use of forward error correction (FEC) and hybrid automatic request (ARQ) mechanisms.* In fact, combined FEC and ARQ strategies can considerably decrease the average number of transmissions. The increasing packet error rate on longer-range underwater links can be compensated for by either decreasing the packet length, or by applying stronger FEC/ARQ schemes.
- 3) *The channel efficiency depends on the packet size and drops with increasing distance.* In particular, i) the average number of packet retransmissions to ensure link reliability increases as the packet size increases, ii) the efficiency decreases as the number of retransmissions increases, and iii) the efficiency increases as the packet payload size increases. Consequently, the optimal packet size is determined in [2] by considering the trade-off between channel efficiency and retransmissions.

To overcome the problems raised by the single-packet transmission scheme, which ultimately lead to low channel efficiencies, we exploit the concept of *packet train*. As shown in Fig. 1, a packet train is a *juxtaposition* of packets that are transmitted *back-to-back* by a node without releasing the channel in a *single atomic transmission*. For delay-insensitive applications, the corresponding node sends for each train an ACK packet, which can either *cumulatively acknowledge* the whole train, i.e., all the consecutively transmitted packets, or it can *selectively* request the retransmission of specific packets (which are then included in the next train). In general, a selective repeat approach is to be preferred.

To the best of our knowledge, this is the first work to

propose this strategy for UW-ASNs, which allows increasing the efficiency of the acoustic channel by increasing the length of the transmitted train without compromising on the packet error rate, i.e., keeping the transmitted packets short. In other words, we *decouple* the effect of the packet size from the choice of the length of the train, i.e., the number of consecutive packets transmitted back-to-back by a node: while the former determines the packet error rate, the latter can be increased as needed in order to increase the channel efficiency. In fact, it is shown in [2] that the channel efficiency associated with the packet-train scheme is,

$$\eta = \eta_T(L_T) \cdot \eta_P(L_P, L_P^F). \quad (2)$$

In (2),  $\eta_T(L_T)$  is the packet-train efficiency, i.e., the ratio between the train payload transmission time and the *train round-trip time*  $T_T^{RTT}$  (Fig. 1) normalized to the bit rate  $r$ ,

$$\eta_T(L_T) = \frac{L_T^D}{L_T^D + L_T^H + L_T^A + r \cdot (2\frac{d}{q} + T_T^{rx-tx})}, \quad (3)$$

where  $L_T$ ,  $L_T^D$ ,  $L_T^H$ , and  $L_T^A$  are the train, payload, header, and ACK length, and  $T_T^{rx-tx}$  is the time needed to process the train and switch the circuitry from receiving to transmitting mode;  $\eta_P(L_P, L_P^F)$  in (2) is the packet efficiency, i.e., the ratio of the packet payload and the packet size multiplied by the average number of transmissions  $\hat{N}^{TX}$  such that a packet is successfully decoded at the receiver,

$$\eta_P(L_P, L_P^F) = \frac{L_P - L_P^H - L_P^F}{\hat{N}^{TX} \cdot L_P}. \quad (4)$$

It can be shown that (4) can also be obtained considering the overhead associated with different retransmission values, i.e., one, two, three, etc., each weighted by its associated probability (which depends on the PER). Due to lack of space, we omit this proof.

Note that, in (3) and (4),  $L_T^A$ ,  $L_T^H$ , and  $L_P^H$  represent system-dependent constants accounting for the length of ACK packets and train and packet headers, while  $L_T$ ,  $L_P$ , and  $L_P^F$  are optimization variables. Also, note that (2) accounts for the decoupling between the train length ( $L_T$ ), which solely affects the train efficiency  $\eta_T$ , and the choice of the packet structure ( $L_P, L_P^F$ ), which solely affects the packet efficiency  $\eta_P$ . Hence, the optimal packet size ( $L_P^*$ ) and optimal FEC redundancy ( $L_P^{F*}$ ) are chosen in such a way as to maximize the packet efficiency  $\eta_P$ , as cast in the optimal packet size problem in [2].

To summarize, the packet size optimization problem finds *off-line* the optimal packet size for delay-insensitive and delay-sensitive applications, whereas the distributed algorithms proposed in the following sections adjust *on-line* the strength of the FEC technique by tuning the amount of FEC redundancy according to the dynamic channel conditions, given the *fixed* packet size  $L_P^*$ . The choice of a fixed packet size for UW-ASNs is motivated by the need for system simplicity and ease of sensor buffer management. In fact, a design proposing per-hop optimal packet size, e.g., solving the packet optimization problem for any link distance and using the resulting *distance-dependent* optimal packet size in the routing algorithms, would encounter several implementation problems, such as the need

for *segmentation* and *re-assembly*, which are functionalities unlikely to be computationally affordable by low-end sensors.

## V. DELAY-INSENSITIVE ROUTING ALGORITHM

In this section, we introduce a distributed geographical routing solution for delay-insensitive underwater applications. Most prior geographical routing protocols assume that nodes can either work in a *greedy mode* or in a *recovery mode*. When in greedy mode, the node that currently holds the message tries to forward it towards the destination. The recovery mode is entered when a node fails to forward a message in the greedy mode as none of its neighbors is a feasible next hop. Usually this occurs when the node - the so-called *concave* node - observes a void region between itself and the destination. Recovery mechanisms, which allow a packet to be forwarded to the destination when a concave node is reached, are out of the scope of this work. The protocol proposed in this section assumes that no void regions exist, although it can be enhanced by combining it with one of the existing recovery mechanisms (e.g., [23], [24]).

The objective of our proposed routing solution is to efficiently exploit the underwater acoustic channel and to minimize the energy consumption. Therefore, the proposed algorithm relies on the packet-train transmission scheme, which is discussed in Sect. IV. In a distributed manner and only exploiting a local view of the network, it allows each node to *jointly* select its best next hop, the transmitted power, and the FEC code rate for each packet, with the objective of minimizing the energy consumption while taking the condition of the underwater channel into account. The algorithm tries to exploit those links that guarantee a low packet error rate in order to maximize the probability that the packet is correctly decoded at the receiver. For these reasons, the energy efficiency of the link is weighted by the number of retransmissions required to achieve link reliability, with the objective of saving energy.

**$\mathbf{P}_{insen}^{\text{dist}}$ : Delay-insensitive Distributed Routing at Node  $i$**

**Given (offline):**  $L_P^*, L_P^H, E_{elec}^b, r, P_{i,max}^{TX}$

**Computed (online):**  $\mathcal{S}_i, \mathcal{P}_i^N, \hat{\Lambda}_{0j}$

**Find:**  $j^* \in \mathcal{S}_i \cap \mathcal{P}_i^N, P_{ij^*}^{TX*} \in [0, P_{i,max}^{TX}],$   
 $L_{P_{ij^*}}^{F*}$

**Minimize:**  $E_i^{(j)} = E_{ij}^b \cdot \frac{L_P^*}{L_P^* - L_P^H - L_{P_{ij}}^F} \cdot$   
 $\hat{N}_{ij}^{TX} \cdot \hat{N}_{ij}^{Hop}$  (5)

**Subject to:**

**(Relationships)**

$$E_{ij}^b = 2 \cdot E_{elec}^b + \frac{P_{ij}^{TX}}{r}; \quad (6)$$

$$L_{P_{ij}}^F = \Psi^{\mathcal{F}-1} \left( L_P^*, PER_{ij}, \Phi^{\mathcal{M}} \left( \frac{P_{ij}^{TX}}{\hat{\Lambda}_{0j} \cdot r \cdot TL_{ij}} \right) \right); \quad (7)$$

$$\hat{N}_{ij}^{TX} = \frac{1}{1 - PER_{ij}}; \hat{N}_{ij}^{Hop} = \max \left( \frac{d_{iN}}{\langle d_{ij} \rangle_{iN}}, 1 \right). \quad (8)$$

Where:

- $L_P^* = L_P^H + L_{P_{ij}}^F + L_{P_{ij}}^N$  [bit] is the *fixed* optimal packet size, where  $L_P^H$  is the *fixed* header size of a packet, while  $L_{P_{ij}}^F$  is the *variable* FEC redundancy that is included in each packet transmitted from node  $i$  to node  $j$ ; thus,  $L_{P_{ij}}^N = L_P^* - L_P^H - L_{P_{ij}}^F$  is the *variable* payload size of each packet transmitted in a train on link  $(i, j)$ .
- $E_{elec}^b = E_{elec}^{trans} = E_{elec}^{rec}$  [J/bit] in (6) is the *distance-independent* energy to transit one bit, where  $E_{elec}^{trans}$  is the energy per bit needed by transmitter electronics (PLLs, VCOs, bias currents, etc.) and digital processing, and  $E_{elec}^{rec}$  represents the energy per bit utilized by receiver electronics. Note that  $E_{elec}^{trans}$  does not represent the overall energy to transmit a bit, but only the *distance-independent* portion of it.
- $E_{ij}^b = 2 \cdot E_{elec}^b + P_{ij}^{TX}/r$  [J/bit] in (6) accounts for the energy to transmit one bit from  $i$  to  $j$ , when the transmitted power and the bit rate are  $P_{ij}^{TX}$  [W] and  $r$  [bps], respectively. The second term represents the *distance-dependent* portion of the energy necessary to transmit a bit.
- $TL_{ij}$  in (7) is the transmission loss (in absolute values and not in dB) from  $i$  to  $j$  (see Sect. III).
- $\hat{N}_{ij}^{TX}$  in (5) and (8) is the average number of transmissions of a packet sent by node  $i$  such that the packet is correctly decoded at receiver  $j$ .
- $\hat{N}_{ij}^{Hop} = \max \left( \frac{d_{iN}}{\langle d_{ij} \rangle_{iN}}, 1 \right)$  in (8) is the estimated number of hops from node  $i$  to the surface station (sink)  $N$  when  $j$  is selected as next hop, where  $d_{ij}$  is the distance between  $i$  and  $j$ , and  $\langle d_{ij} \rangle_{iN}$  (which we refer to as *advance*) is the projection of  $d_{ij}$  onto the line connecting node  $i$  with the sink.
- $BER_{ij} = \Phi^{\mathcal{M}} \left( \frac{P_{ij}^{TX}}{\hat{\Lambda}_{0j} \cdot r \cdot TL_{ij}} \right)$  in (7) represents the bit error rate on link  $(i, j)$ ; it is a function of the ratio between the energy of the received bit,  $E_{rec}^b = P_{ij}^{TX}/(r \cdot TL_{ij})$ , and the expected noise at node  $j$ ,  $\hat{\Lambda}_{0j}$ , and it depends on the adopted modulation scheme  $\mathcal{M}$ .
- $L_{P_{ij}}^F = \psi^{\mathcal{F}-1} (L_P^*, PER_{ij}, BER_{ij})$  in (7) returns the needed FEC redundancy, given the optimal packet size  $L_P^*$ , the packet error rate and bit error rate on link  $(i, j)$ , and it depends on the adopted FEC technique  $\mathcal{F}$ . Note that, similarly, the packet error rate depends on the FEC technique, the packet length, the bit error rate, and the FEC redundancy, i.e.,  $PER_{ij} = \psi^{\mathcal{F}} (L_P^*, BER_{ij}, L_{P_{ij}}^F)$ .
- $\mathcal{S}_i$  is the *neighbor set* of node  $i$ , while  $\mathcal{P}_i^N$  is the *positive advance set*, composed of nodes closer to sink  $N$  than node  $i$ , i.e.,  $j \in \mathcal{P}_i^N$  iff  $d_{jN} < d_{iN}$ .

According to the proposed algorithm for delay-insensitive applications, node  $i$  will select  $j^*$  as its best next hop iff

$$j^* = \arg \min_{j \in \mathcal{S}_i \cap \mathcal{P}_i^N} E_i^{(j)*}, \quad (9)$$

where  $E_i^{(j)*}$  represents the minimum energy required to successfully transmit a payload bit from node  $i$  to the sink, taking the condition of the underwater channel into account, when  $i$  selects  $j$  as next hop. This link metric, objective function (5) in  $\mathbf{P}_{insen}^{\text{dist}}$ , takes into account the number of packet transmissions ( $\hat{N}_{ij}^{TX}$ ) associated with link  $(i, j)$ , given the optimal packet size ( $L_P^*$ ), and the optimal combination

of FEC ( $L_{Pij}^{F*}$ ) and transmitted power ( $P_{ij}^{TX*}$ ). Moreover, it accounts for the average hop-path length ( $\hat{N}_{ij}^{Hop}$ ), which is the estimated number of hops from node  $i$  to the surface station when  $j$  is selected as next hop, assuming that the following hops will guarantee the same advance towards the surface station. This estimate has three properties: 1) it does not incur any signaling overhead as it is locally computed and does not require end-to-end information exchange, 2) its accuracy increases as the density increases, and 3) as the distance between the surface station and the current node decreases.

The link metric  $E_i^{(j)*}$  in (9) represents the optimal energy per payload bit when  $i$  transmits a packet train to  $j$  using the optimal combination of power  $P_{ij}^{TX*}$  and FEC redundancy  $L_{Pij}^{F*}$  to achieve link reliability, jointly found by solving problem  $\mathbf{P}_{insen}^{dist}$ . This allows node  $i$  to optimally decouple  $\mathbf{P}_{insen}^{dist}$  into two *sub-problems*: *first*, minimize the link metric  $E_i^{(j)}$  for each of its feasible next-hop neighbors; *second*, pick as best next hop that node  $j^*$  associated with the minimal link metric. This means that the generic node  $i$  does not have to solve a complicated optimization problem to find its best route towards a sink. Rather, it only needs to sequentially solve the two aforementioned low-complexity subproblems, each characterized by a complexity  $O(|\mathcal{S}_i \cap \mathcal{P}_i^N|)$ , i.e., proportional to the number of its neighboring nodes with positive advance towards the sink. Moreover, this operation does not need to be performed each time a sensor has to route a packet, but only when the channel conditions have changed.

Note that the proposed algorithm considers the effect of the *bandwidth-distance relationship* that is captured by the transmission loss ( $TL_{ij}$ ) in (7), which affects the bit error rate ( $BER_{ij}$ ). This, in turn, affects the packet error rate ( $PER_{ij}$ ), and ultimately the number of packet transmissions ( $\hat{N}_{ij}^{TX}$ ), as accounted for in (8).

To summarize, the proposed routing solution allows node  $i$  to select as next hop that node  $j^*$  among its neighbors that satisfies the following two requirements: 1) it is closer to the surface station than  $i$ , and 2) it minimizes the link metric  $E_i^{(j)*}$ . While this heuristic approach does not guarantee global optimality as a sender does not have a global view of the network, it achieves the ‘best’ possible performance given the limited information at the sender.

## VI. DELAY-SENSITIVE ROUTING ALGORITHM

Similarly to the delay-insensitive algorithm introduced in Sect. V, the delay-sensitive routing algorithm allows each node to select in a distributed manner the optimal next hop, transmit power, and FEC packet rate with the objective of minimizing the energy consumption. *However, this algorithm includes two new constraints to statistically meet the delay-sensitive application requirements:*

- 1) The end-to-end packet error rate should be lower than an application-dependent threshold  $PER_{max}^{e2e}$ ;
- 2) The probability that the end-to-end packet delay be over a delay bound  $B_{max}$ , should be lower than an application-dependent parameter  $\gamma$ .

As a design guideline to meet these requirements, differently from the routing algorithm tailored for delay-insensitive applications, the proposed algorithm does not retransmit lost

or corrupted packets at the link layer. Moreover, it time-stamps packets when they are generated by a source so that they can be discarded when they expire. To save energy, while statistically limiting the end-to-end packet delay, we rely on an *earliest deadline first* scheduling, which dynamically assigns higher priority to packets closer to their deadline.

$\mathbf{P}_{sen}^{dist}$ : **Delay-sensitive Distributed Routing at Node  $i$**

$$\textbf{Given (offline): } L_P^*, L_P^H, M = \lfloor \frac{L_T^* - L_T^H}{L_P^*} \rfloor, E_{elec}^b, r, P_{i,max}^{TX}$$

$$\textbf{Computed (online): } \mathcal{S}_i, \mathcal{P}_i^N, \hat{\Lambda}_{0j}, \Delta B_i^{(m)}, \hat{Q}_{ij}$$

$$\textbf{Find: } j^* \in \mathcal{S}_i \cap \mathcal{P}_i^N, P_{ij^*}^{TX*} \in [0, P_{i,max}^{TX}], L_{Pij^*}^{F*}$$

$$\textbf{Minimize: } E_i^{(j)} = E_{ij}^b \cdot \frac{L_P^*}{L_P^* - L_P^H - L_{Pij}^F} \cdot \hat{N}_{ij}^{Hop} \quad (10)$$

**Subject to:**

**(Relationships)**

$$E_{ij}^b = 2 \cdot E_{elec}^b + \frac{P_{ij}^{TX}}{r}; \quad (11)$$

$$L_{Pij}^F = \Psi^{\mathcal{F}^{-1}} \left( L_P^*, PER_{ij}, \Phi^{\mathcal{M}} \left( \frac{P_{ij}^{TX}}{\hat{\Lambda}_{0j} \cdot r \cdot TL_{ij}} \right) \right); \quad (12)$$

$$\hat{N}_{ij}^{Hop} = \max \left( \frac{d_{iN}}{\langle d_{ij} \rangle_{iN}}, 1 \right); \quad (13)$$

**(Constraints)**

$$1 - \left( 1 - PER_{ij} \right)^{\lceil \hat{N}_{ij}^{Hop} \rceil} \leq PER_{max}^{e2e}; \quad (14)$$

$$\frac{\tilde{d}_{ij}}{Q_{ij}} + \delta(\gamma) \cdot \sigma_{ij}^q \leq \min_{m=1, \dots, M} \left( \frac{\Delta B_i^{(m)}}{\hat{N}_{ij}^{Hop}} \right) - \hat{Q}_{ij} - \frac{L_P^*}{r}. \quad (15)$$

In the following, we introduce the new notations used in the delay-sensitive problem formulation:

- $M = \lfloor (L_T^* - L_T^H) / L_P^* \rfloor$  in (15) is the *fixed* number of packets transmitted in a train on each link, where  $L_T^*$  and  $L_P^*$  are the optimal train length and packet size, respectively, as discussed in Sect. IV.
- $PER_{max}^{e2e}$  in (14) and  $B_{max}$  [s] are the application-dependent end-to-end packet error rate and delay bounds, respectively.
- $\Delta B_i^{(m)} = B_{max} - [t_{i,now}^{(m)} - t_0^{(m)}]$  [s] in (15) is the time-to-live of packet  $m$  arriving at node  $i$ , where  $t_{i,now}^{(m)}$  is the arriving time of  $m$  at  $i$ , and  $t_0^{(m)}$  is the time  $m$  was generated, which is time-stamped in the packet header by its source.
- $T_{ij} = L_P^* / r + T_{ij}^q$  [s] accounts for the packet transmission and propagation delay associated with link  $(i, j)$ , as described in Sect. III; according to measurements on underwater channels reporting a symmetric delay distribution of multipath rays [5], we consider a Gaussian distribution for  $T_{ij}$ , i.e.,  $T_{ij} \sim \mathcal{N}(L_P^* / r + \overline{T}_{ij}^q, \sigma_{ij}^q{}^2)$ .
- $\hat{Q}_{ij}$  [s] in (15) is the network queueing delay estimated by node  $i$  when  $j$  is selected as next hop, computed according to the information carried by incoming packets and broadcast by neighboring nodes, as will be detailed in the next section.

The formulation of  $\mathbf{P}_{sen}^{dist}$  is quite similar to  $\mathbf{P}_{insen}^{dist}$ , except for two important differences:

- 1) The objective function (10) does not include  $\hat{N}_{ij}^{TX}$  as

no selective packet retransmission is performed;

- 2) Two new constraints are included, (14) and (15), which address the two considered delay-sensitive application requirements.

Note that (14) forces the packet error rate  $PER_{ij}$  that will be experienced by packet  $m$  on link  $(i, j)$  to respect the application end-to-end packet error rate requirement ( $PER_{max}^{e2e}$ ), given the estimated number of hops to reach the sink if  $j$  is selected as next hop ( $\hat{N}_{ij}^{Hop}$ ). Interestingly, because the packet is assumed to be correctly forwarded up to node  $i$ , there is no need to consider the hop count number in (14), i.e., the number of hops of packet  $m$  from the source to the current node  $i$ . In fact, as node  $i$  is assumed to receive the packet, the conditional probability of it being correct is one. Consequently, the further node  $i$  is from the destination (in terms of expected number of hops), the lower the tolerated link packet error rate on link  $(i, j^*)$  is. As far as Constraint (15) is concerned, its mathematical derivation is provided in the following section. Note that the complexity of  $\mathbf{P}_{sen}^{dist}$  is  $O(|\mathcal{S}_i \cap \mathcal{P}_i^N|)$ , i.e., proportional to the number of neighboring nodes with positive advance towards the sink.

### Statistical Link Delay Model

In this section, we derive constraint (15) in  $\mathbf{P}_{sen}^{dist}$  that each link needs to meet in order to statistically bound the end-to-end packet delay. To this end, we model the propagation delay of each link  $(i, j)$  as a random variable  $T_{ij}^q$ , with mean equal to  $\overline{T_{ij}^q}$  and variance  $\sigma_{ij}^q$ . The mean  $\overline{T_{ij}^q} = \tilde{d}_{ij}/\overline{q_{ij}}$  is computed as the ratio of the average multiple path length  $\tilde{d}_{ij}$  and the average underwater propagation speed of an acoustic wave propagating from node  $i$  to node  $j$  (see Sect. III). In vertical links, sound rays propagate directly without bouncing at the bottom or surface of the ocean. Hence, the multipath effect is negligible, and  $\tilde{d}_{ij} \approx d_{ij}$ . Conversely, in shallow-water horizontal links, potentially tens or hundreds of rays propagate by bouncing at the bottom and surface of the ocean along with the direct ray. Consequently,  $\tilde{d}_{ij}$  is generally much larger than  $d_{ij}$ . This is due to the fact that in state-of-the-art underwater receivers, multipath can be compensated for by waiting for the energy spread on multiple non-direct rays. In this way, it is possible to capture the energy spread on multiple paths, and thus guarantee a higher SNR given a fixed transmit power. However, the price for this compensation is that the end-to-end delay is affected by the propagation delay of several rays.

Given the statistical properties of underwater links, we want the probability that a packet exceed its end-to-end delay bound  $B_{max}$  to be lower than an application-dependent fixed parameter  $\gamma$ . Hence, it should hold

$$\begin{aligned} \Pr \left\{ [t_{i,now}^{(m)} - t_0^{(m)}] + B_{iN}^{(j)} \geq B_{max} \right\} &= \\ &= \Pr \left\{ B_{iN}^{(j)} \geq \Delta B_i^{(m)} \right\} \leq \gamma, \end{aligned} \quad (16)$$

where  $B_{iN}^{(j)}$  is the expected delay a packet will incur from node  $i$  to the surface station  $N$  when  $j$  is chosen as next hop, and  $\Delta B_i^{(m)} = B_{max} - [t_{i,now}^{(m)} - t_0^{(m)}]$  is the time-to-live of packet  $m$  arriving at node  $i$ . Node  $i$  can estimate the remaining path

delay by projecting, for each possible next hop  $j$ , the estimated network queueing delay  $\hat{Q}_{ij}$  and the transmission delay  $T_{ij}$  to the remaining hops  $\hat{N}_{ij}^{Hop}$ , i.e.,

$$B_{iN}^{(j)} \approx (T_{ij} + \hat{Q}_{ij}) \cdot \hat{N}_{ij}^{Hop}, \quad (17)$$

where

$$\hat{Q}_{ij} = \frac{t_{i,now}^{(m)} - t_0^{(m)} - \sum_{(k,h) \in \mathcal{L}_i^{(m)}} \overline{T}_{kh} + \overline{Q}_i + \overline{Q}_j}{N_{HC}^{(m)} + 2}. \quad (18)$$

In (18), the estimated network queueing delay  $\hat{Q}_{ij}$  is computed as the ratio of the sum of all the queueing delays experienced by packet  $m$  along its path  $\mathcal{L}_i^{(m)}$ , which includes the links from the source generating packet  $m$  to node  $i$ , and the average queueing delays  $\overline{Q}_i$ , measured by node  $i$ , and  $\overline{Q}_j$ , periodically broadcast by  $j$ ; and the number of nodes forwarding the packet, including node  $i$ , which depends on the hop count  $N_{HC}^{(m)}$  (which is the number of hops of packet  $m$  from the source to the current node).

By substituting (17) into (16), and by assuming a Gaussian distribution for  $T_{ij}$ , (16) can be rewritten as

$$\begin{aligned} \Pr \left\{ T_{ij} \geq \frac{\Delta B_i^{(m)}}{\hat{N}_{ij}^{Hop}} - \hat{Q}_{ij} \right\} &= \\ &= \frac{1}{2} \left[ 1 - \operatorname{erf} \left( \frac{\frac{\Delta B_i^{(m)}}{\hat{N}_{ij}^{Hop}} - \hat{Q}_{ij} - \overline{T}_{ij}}{\sqrt{2} \cdot \sigma_{ij}^q} \right) \right] \leq \gamma, \end{aligned} \quad (19)$$

where the  $\operatorname{erf}(\Gamma)$  function is defined as  $\operatorname{erf}(\Gamma) = \frac{2}{\sqrt{\pi}} \cdot \int_0^\Gamma e^{-t^2} dt$ . Because  $\overline{T}_{ij} = L_P^*/r + \overline{T_{ij}^q}$ , and  $\overline{T_{ij}^q} = \tilde{d}_{ij}/\overline{q_{ij}}$ , (19) simplifies to

$$\frac{\tilde{d}_{ij}}{\overline{q_{ij}}} + \delta(\gamma) \cdot \sigma_{ij}^q \leq \frac{\Delta B_i^{(m)}}{\hat{N}_{ij}^{Hop}} - \hat{Q}_{ij} - \frac{L_P^*}{r}, \quad (20)$$

where  $\delta(\gamma) = \sqrt{2} \cdot \operatorname{erf}^{-1}(1 - 2\gamma)$  only depends on  $\gamma$ . In particular,  $\delta(\gamma)$  increases with decreasing values of  $\gamma$ . In addition, in order to consider, as a precautionary guideline, the tightest constraint among all those associated with the  $M$  packets to be transmitted in a train, a 'min' operator is added to the right-hand side of (20), which leads to (15). Note that, while constraint (15) does not bound the delay of a packet, it increases the probability that a packet can reach the sink within its delay bound. To achieve this, the proposed algorithm only relies on the past access delay information carried by the packet, and on information about its 1-hop neighborhood, and not on end-to-end signaling. This information is obtained by broadcast messages. However, to limit the overhead caused by these messages, each node advertises its access delay only when it exceeds a pre-defined threshold. Hence, this mechanism allows the routing algorithm to dynamically adapt to the ongoing traffic and the resulting congestion.

## VII. PERFORMANCE EVALUATION

We present the simulation performance of the proposed routing solutions for delay-insensitive and delay-sensitive UW-ASN applications, introduced in Sects. V and VI, respectively.

TABLE I  
SIMULATION PARAMETERS FOR SCENARIOS 1, 2, AND 3

	Scen. 1	Scen. 2	Scen. 3
App. Type [Delay-]	insensitive	insensitive	sensitive
Traffic Type	background	event	event
No. of Sources	100	15	15
Volume [Km <sup>3</sup> ]	.1x.1x.1	.5x.5x.05	.5x.5x.05
Packet Size [KByte]	.5	.5	.1
Source Rate [Kbps]	.01	.15, .3, .6	.15, .3, .6
Max. TX Power [W]	.5	5	5

We extended the wireless package of the J-Sim simulator [25], which implements the whole protocol stack of a sensor node, to simulate the characteristics of the 3D underwater environment. We modeled the underwater transmission loss, the transmission and propagation delays of vertical and horizontal links, and the physical layer characteristics of underwater receivers. As far as the MAC layer is concerned, we adapted the behavior of IEEE 802.11 to the underwater environment to emulate MAC protocols implemented by leading underwater acoustic modems such as WHOI and Benthos. Firstly, we disabled the RTS/CTS handshaking, as it yields high delays in a low-bandwidth high-delay environment and it solves neither the hidden nor the exposed terminal problems due the uncorrelated states of the channel at the transmitter and at the receiver. Secondly, we tuned all the parameters of IEEE 802.11 according to the physical layer characteristics. For example, the value of the *slot time* in the 802.11 backoff mechanism has to account for the propagation delay at the physical layer [26]. Hence, while it is set to 20  $\mu$ s for terrestrial 802.11 Direct Sequence Spread Spectrum (DSSS), we experimented that a value of 0.18 s is needed to allow devices a few hundred meters apart to share the underwater medium. This implies that the delay introduced by the backoff contention mechanism is several orders of magnitude higher than in terrestrial channels, which in turn leads to low channel utilizations. For this reason, we set the values of the contention windows  $CW_{min}$  and  $CW_{max}$  [26] to 4 and 32, respectively, whereas in 802.11 DSSS they are set to 32 and 1024.

We performed three sets of experiments to analyze the performance of the proposed routing solutions. The main parameters differentiating the three experimental scenarios are summarized in Table I, while the common parameters are reported hereafter: 100 sensors are randomly deployed in a 3D volume, the initial node energy is set to 1000 J, and the available bandwidth is 50 kHz. In Scenario 1, presented in Sect. VII-A, all deployed sensors are low-rate sources, which allows us to simulate a *low-intensity delay-insensitive background monitoring traffic* from a small 3D volume (100x100x100 m<sup>3</sup>). Conversely, in Scenarios 2 and 3, presented in Sect. VII-B, we compare the delay-insensitive and delay-sensitive routing algorithms when 100 sensors are randomly deployed in a larger 3D volume (500x500x50 m<sup>3</sup>), which may represent a small harbor. Note that, differently from Scenario 1, in these sets of experiments only some sen-

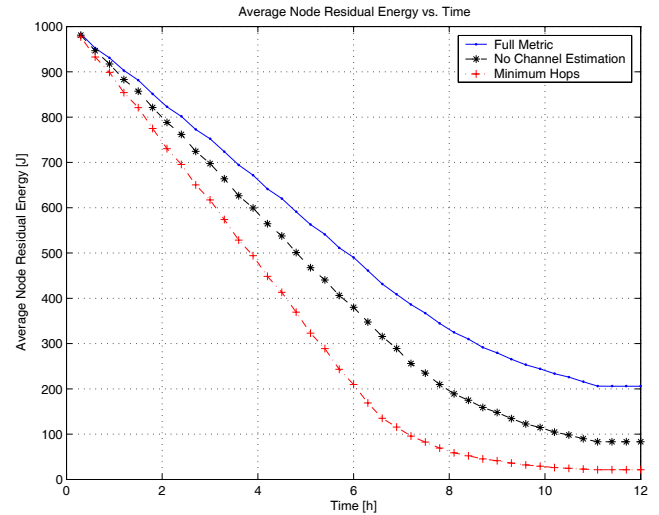


Fig. 2. **Scenario 1: Delay-insensitive routing.** Average node residual energy vs. time, for different link metrics.

TABLE II  
SCENARIO 1- DELAY-INSENSITIVE ROUTING: AVERAGE AND STANDARD DEVIATION OF NO. OF HOPS (WITH CONFIDENCE INTERVALS)

	Full Metric	No Channel	Min. Hops
Average	$2.3 \pm 1.1$	$1.2 \pm 0.3$	$1.2 \pm 0.3$
Std	$1.3 \pm 0.2$	$0.4 \pm 0.2$	$0.2 \pm 0.1$

sors inside an event area of spherical radius 100 m (centered inside the 3D monitoring volume) are sources of data packets of size equal to 500 and 100 Bytes for delay-insensitive and delay-sensitive applications, respectively.

#### A. Scenario 1: Delay-insensitive Background Traffic

We considered 100 sensors randomly deployed in a small 3D volume of 100x100x100 m<sup>3</sup>. We set the maximum transmission power to 0.5 W and the packet size to 500 Bytes. All deployed sensors are low-rate sources, which allows us to simulate a low-intensity background monitoring traffic from the entire volume, i.e., each node transmits a data packet every 600 s.

In Fig. 2 we show the average node residual energy over the simulation time. In particular, we compare the routing performance when three different link metrics are used. Specifically, our *Full Metric* as in (5), introduced in Sect. V; the *No Channel Estimation*, which does not consider the channel condition, i.e., does not take the expected number of packet transmissions ( $\hat{N}^{TX}$ ) into account; and the *Minimum Hops*, which simply minimizes the number of hops to reach the surface station. When the channel state condition is considered (Full Metric), considerable energy savings can be achieved, which is expected to lead to prolonged network lifetime.

In Table II, we present the average number of hops and the standard deviation of the number of hops (computed among all the nodes in the network) when the different link metrics are used. In the table, we also provide the 95% confidence intervals associated with both measurements; these intervals

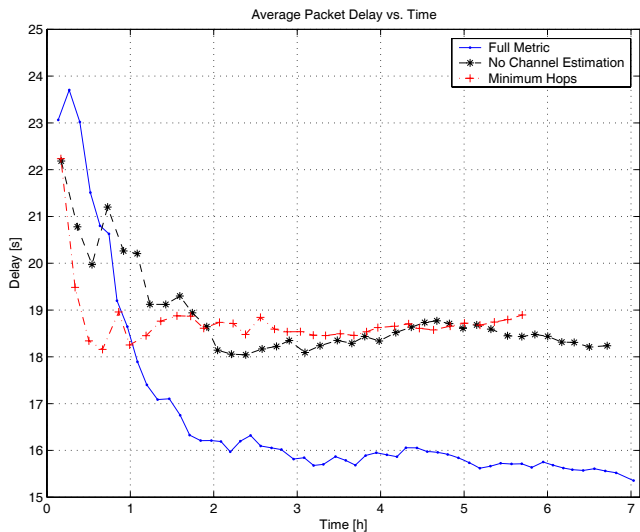


Fig. 3. **Scenario 1: Delay-insensitive routing.** Average packet delay vs. time, for different link metrics.

are computed across multiple simulation runs for statistical purpose.

In Fig. 3, we show the trend of the average packet delays over time when the different link metrics are used. The packet delay accounts for the time the network takes to transmit a packet from the source node to the destination node (possibly following a multi-hop path where other nodes in the network act as relays); hence, this metric incorporates all the intermediate delays (e.g., transmitting a packet on a link, processing at a relay node, retransmitting on another link, and so on until the packet reaches the destination). In the figure, we show the average packet delay, which is computed by averaging the above packet-specific metric among all the packets received by the sink. Note that the average packet delay associated with any metric decreases in time during a transient phase, until converging to a steady-state value. This phenomenon can be explained by the fact that nodes desynchronize their transmissions as time progresses, which leads to less packet collisions and, consequently, to less packet retransmissions at the link layer.

By comparing the path lengths and the average end-to-end packet delay results, we can conclude that when our full link metric is adopted (i.e., the Full Metric), packet delays are smaller than with the other metrics, although the data paths chosen are longer. A lower number of packet transmissions is to be expected as the full metric takes the state of the underwater channel into account. Hence, next hops associated with better channels are selected. This, in turn, reduces the average queuing delays as packets are less likely to be retransmitted.

### B. Scenarios 2 and 3: Comparison Between Delay-insensitive and Delay-sensitive Event-driven Traffic

We compared the delay-insensitive and delay-sensitive routing algorithms when 100 sensors are randomly deployed in a 3D volume of  $500 \times 500 \times 50 \text{ m}^3$ . Differently from the previous scenario, only some sensors inside a spherical event area of radius 100 m (centered inside the 3D monitoring volume)

are sources of data packets of size equal to 500 and 100 Bytes for delay-insensitive and delay-sensitive applications, respectively. In these simulation scenarios, we incorporated the effect of the fast fading Rayleigh channel (coherence time set to 0.5 s) to capture the heavy multipath environment in shallow water (depth equal to 50 m). In these experiments we set the maximum transmit power to 5 W, as reported in Table I, to account for the larger network diameter than in Scenario 1, i.e., 700 vs. 170 m. We performed three sets of experiments, each using different source data rates, 150, 300, and 600 bps.

Figure 4 reports the end-to-end packet delay and average delay (a more stable average delay computed using a sliding window that filters out some of the fluctuations in the packet delay metric) over time for the three considered source rates for delay-insensitive traffic (Scenario 2), while Fig. 5 shows the same metrics for delay-sensitive traffic (Scenario 3). From these experiments, we notice that when the source data rate increases, the delay-sensitive routing algorithm can statistically bound the end-to-end delay, as shown in Figs. 5(a-c), where the delays are always smaller than fractions of second. Conversely, the delay-insensitive routing algorithm results in high average and peak delays, as can be seen in Figs. 4(b-c). The delay-sensitive routing algorithm can statistically bound the delay as next-hop nodes are chosen in such a way as to control the delay dispersion on each link, as captured by constraint (15) of  $\mathbf{P}_{\text{sens}}^{\text{dist}}$  (Sect. VI). Furthermore, expired packet(s) are discarded in order to not waste bandwidth. As opposed to the delay-insensitive routing algorithm, which manages to deliver all the generated traffic at the expenses of packet delays, corrupted packets carrying delay-sensitive data are not retransmitted, which is reflected in the small sensor queue size. While in Scenario 2 tens of packets are on average enqueued by sensor nodes, in Scenario 3 only a few packets fill the queues. Table III reports the surface station (sink) and node average energy expenditure per correctly received bit for the three different source data rates. Interestingly, in both scenarios the minimum sink and average energy per bit (in the order of tens of  $\mu\text{J}/\text{bit}$ ) is associated with the intermediate data rate, i.e., 300 bps, when sources generate a consistent amount of traffic without causing network congestion. In addition, due to packet retransmissions, in Scenario 2 the energy per bit dissipated by relaying nodes is almost the same as that required by the surface station to receive and acknowledge incoming packets. Conversely, a remarkable difference between surface station and average node energy per bit can be noticed in Scenario 3, where the phenomenon of *traffic concentration* at the surface station prevails as far as the total amount of dissipated energy in the network is concerned.

## VIII. CONCLUSIONS

The problem of data gathering in a 3D underwater acoustic sensor network was investigated by considering the interactions between the routing functions and the signal propagation characteristics in the underwater environment. Two distributed geographical routing algorithms for delay-insensitive and delay-sensitive applications were introduced and evaluated through simulations; their objective is to minimize the energy consumption while taking the varying condition of

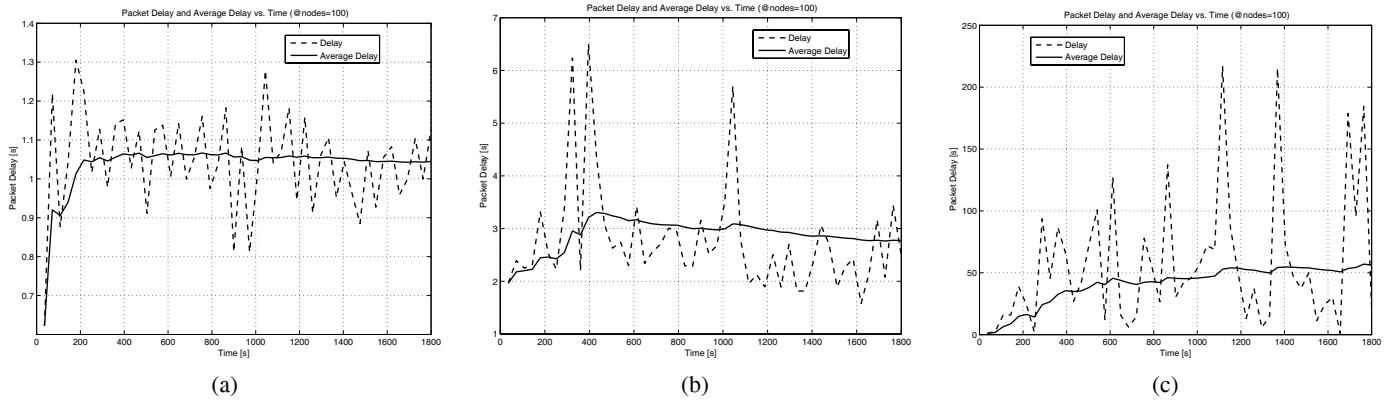


Fig. 4. **Scenario 2: Delay-insensitive routing.** Packet delay and average delay vs. time for three source rates. (a): Source rate equal to 150 bps; (b): Source rate equal to 300 bps; (c): Source rate equal to 600 bps.

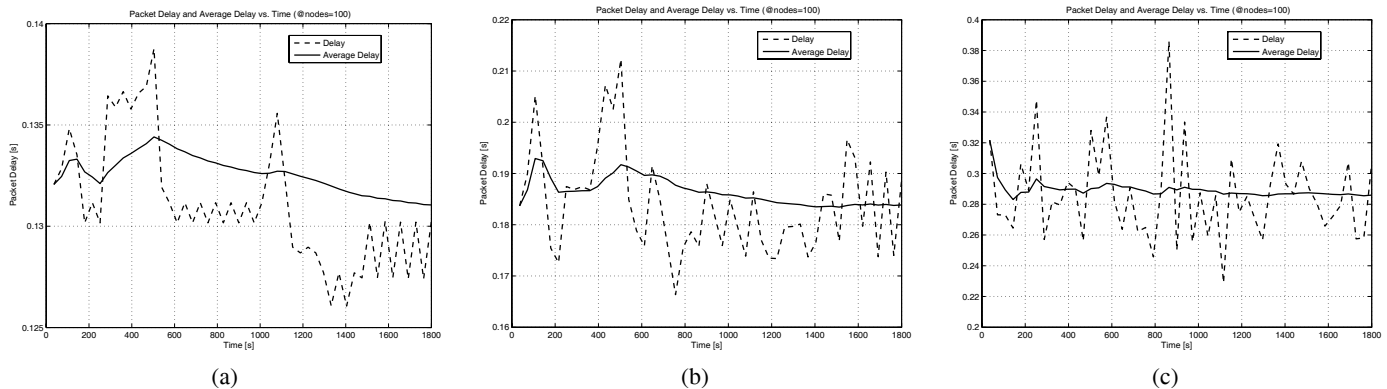


Fig. 5. **Scenario 3: Delay-sensitive routing.** Packet delay and average delay vs. time for three source rates. (a): Source rate equal to 150 bps; (b): Source rate equal to 300 bps; (c): Source rate equal to 600 bps.

TABLE III

SCENARIOS 2 AND 3: SURFACE STATION AND NODE AVERAGE ENERGY EXPENDITURE PER BIT [ $\mu\text{J}/\text{bit}$ ] (WITH CONFIDENCE INTERVALS)

Source Rate [bps]	150	300	600
Scen. 2. Surface Station	$8 \pm 1.4$	$6.5 \pm 0.9$	$7.5 \pm 1.2$
Scen. 2. Node Average	$7 \pm 1.0$	$4 \pm 0.6$	$5.5 \pm 0.8$
Scen. 3. Surface Station	$21 \pm 3.1$	$17 \pm 2.7$	$18 \pm 2.9$
Scen. 3. Node Average	$9 \pm 1.4$	$6 \pm 0.8$	$5 \pm 0.6$

the underwater acoustic channel and the different application requirements into account.

## REFERENCES

- [1] I. F. Akyildiz, D. Pompili, and T. Melodia, "Underwater acoustic sensor networks: research challenges," *Ad Hoc Netw.* (Elsevier), vol. 3, no. 3, pp. 257-279, May 2005.
- [2] D. Pompili, T. Melodia, and I. F. Akyildiz, "Routing algorithms for delay-insensitive and delay-sensitive applications in underwater sensor networks," in *Proc. ACM Conf. Mobile Comput. Netw. (MobiCom)*, Los Angeles, CA, Sep. 2006.
- [3] A. F. Harris III and M. Zorzi, "Energy-efficient routing protocol design considerations for underwater networks," in *Proc. IEEE Conf. Sensor, Mesh Ad Hoc Commun. Netw. (SECON)*, San Diego, CA, June 2007.
- [4] J. Proakis, E. Sozer, J. Rice, and M. Stojanovic, "Shallow water acoustic networks," *IEEE Commun. Mag.*, pp. 114-119, Nov. 2001.
- [5] M. Stojanovic, "Acoustic (underwater) communications," *Encyclopedia of Telecommun.*, J. G. Proakis, editor. John Wiley and Sons, 2003.
- [6] —, "On the relationship between capacity and distance in an underwater acoustic communication channel," in *Proc. ACM International Workshop UnderWater Netw. (WUWNet)*, Los Angeles, CA, Sep. 2006.
- [7] D. Pompili and I. F. Akyildiz, "A cross-layer communication solution for multimedia applications in underwater acoustic sensor networks," in *Proc. IEEE International Conf. Mobile Ad-hoc Sensor Syst. (MASS)*, Atlanta, GA, Sep. 2008.
- [8] E. Sozer, J. Proakis, M. Stojanovic, J. Rice, A. Benson, and M. Hatch, "Direct sequence spread spectrum based modem for underwater acoustic communication and channel measurements," in *Proc. MTS/IEEE Conf. Exhibition Ocean Eng., Science Technol. (OCEANS)*, Seattle, WA, Nov. 1999.
- [9] M. Abolhasan, T. Wysocki, and E. Dutkiewicz, "A review of routing protocols for mobile ad hoc networks," *Ad Hoc Netw.* (Elsevier), vol. 2, pp. 1-22, Jan. 2004.
- [10] K. Akkaya and M. Younis, "A survey on routing protocols for wireless sensor networks," *Ad Hoc Netw.* (Elsevier), vol. 3, no. 3, pp. 325-349, May 2005.
- [11] T. Melodia, D. Pompili, and I. F. Akyildiz, "On the interdependence of distributed topology control and geographical routing in ad hoc and sensor networks," *IEEE J. Sel. Areas Commun.*, vol. 23, no. 3, pp. 520-532, Mar. 2005.
- [12] V. Chandrasekhar, W. K. Seah, Y. S. Choo, and H. V. Ee, "Localization in underwater sensor networks—survey and challenges," in *Proc. ACM International Workshop UnderWater Netw. (WUWNet)*, Los Angeles, CA, Sep. 2006.
- [13] G. Xie and J. Gibson, "A network layer protocol for UANs to address propagation delay induced performance limitations," in *Proc. MTS/IEEE Conf. Exhibition Ocean Eng., Science Technol. (OCEANS)*, vol. 4, Honolulu, HI, Nov. 2001, pp. 2087-2094.
- [14] D. Pompili, T. Melodia, and I. F. Akyildiz, "A resilient routing algorithm for long-term applications in underwater sensor networks," in *Proc. Mediterranean Ad Hoc Netw. Workshop (Med-Hoc-Net)*, Lipari, Italy, June 2006.
- [15] P. Xie, J.-H. Cui, and L. Lao, "VBF: vector-based forwarding protocol

for underwater sensor networks," in *Proc. Netw.*, Coimbra, Portugal, May 2006.

- [16] W. Zhang and U. Mitra, "A delay-reliability analysis for multihop underwater acoustic communication," in *Proc. ACM International Workshop UnderWater Netw. (WUWNet)*, Montreal, Quebec, Canada, Sep. 2007.
- [17] E. Sozer, M. Stojanovic, and J. Proakis, "Underwater acoustic networks," *IEEE J. Oceanic Eng.*, vol. 25, no. 1, pp. 72-83, Jan. 2000.
- [18] I. Vasilescu, K. Kotay, D. Rus, M. Dunbabin, and P. Corke, "Data collection, storage, and retrieval with an underwater sensor network," in *ACM Conf. Embedded Netw. Sensor Syst. (SenSys)*, San Diego, CA, Nov. 2005.
- [19] A. Nimbalkar and D. Pompili, "Reliability in underwater inter-vehicle communications," in *Proc. ACM International Workshop UnderWater Netw. (WUWNet)*, San Francisco, CA, Sep. 2008.
- [20] D. Pompili, T. Melodia, and I. F. Akyildiz, "Deployment analysis in underwater acoustic wireless sensor networks," in *Proc. ACM International Workshop UnderWater Netw. (WUWNet)*, Los Angeles, CA, Sep. 2006.
- [21] R. J. Urick, *Principles of Underwater Sound*. McGraw-Hill, 1983.
- [22] M. Stojanovic, "Optimization of a data link protocol for an underwater acoustic channel," in *Proc. MTS/IEEE Conf. Exhibition Ocean Eng., Science Technol. (OCEANS)*, Brest, France, June 2005.
- [23] B. Karp and H. Kung, "GPSR: greedy perimeter stateless routing for wireless networks," in *Proc. ACM Conf. Mobile Comput. Netw. (MobiCom)*, Boston, MA, Aug. 2000, pp. 243-254.
- [24] P. Bose, P. Morin, I. Stojmenovic, and J. Urrutia, "Routing with guaranteed delivery in ad hoc wireless networks," *ACM-Kluwer Wireless Netw.* (Springer), vol. 7, no. 6, pp. 609-616, Nov. 2001.
- [25] The J-Sim Simulator. [Online]. Available: <http://www.j-sim.org/>.
- [26] G. Bianchi, "Performance analysis of the IEEE 802.11 DCF," *IEEE J. Sel. Areas Commun.*, vol. 18, no. 3, pp. 535-547, Mar. 2000.



**Dario Pompili** joined the faculty of the Department of Electrical and Computer Engineering at Rutgers, The State University of New Jersey, as Assistant Professor in Fall 2007. He received his Ph.D. in Electrical and Computer Engineering from the Georgia Institute of Technology in June 2007 after working at the Broadband Wireless Networking Laboratory (BWN-Lab) directed by Prof. I. F. Akyildiz. In 2005, he was awarded Georgia Institute of Technology BWN-Lab Researcher of the Year for "outstanding contributions and professional achievements." He had previously received his 'Laurea' (integrated B.S. and M.S.) and Doctorate degrees in Telecommunications Engineering and System Engineering from the University of Rome "La Sapienza," Italy, in 2001 and 2004, respectively. His research interests include ad hoc and sensor networks, underwater acoustic communications, wireless sensor and actor networks, and network optimization and control. He is author and co-author of many influential publications in these fields. He is in the editorial board of the journal *Ad Hoc Networks* (Elsevier) and in the technical program committee of several leading conferences on networking. He is also member of the IEEE Communications Society and the ACM.



**Tommaso Melodia** (M'2007) (tmelodia@eng.buffalo.edu) is an Assistant Professor with the Department of Electrical Engineering at the University at Buffalo, The State University of New York (SUNY), where he directs the Wireless Networks and Embedded Systems Laboratory. He received his Ph.D. in Electrical and Computer Engineering from the Georgia Institute of Technology in June 2007. He had previously received his "Laurea" (integrated B.S. and M.S.) and Doctorate degrees in Telecommunications

Engineering from the University of Rome "La Sapienza," Rome, Italy, in 2001 and 2005, respectively. He is the recipient of the BWN-Lab Researcher of the Year award for 2004. He coauthored a paper that was recognized as the *Fast Breaking Paper in the field of Computer Science* for February 2009 by Thomson ISI Essential Science Indicators. He is an Associate Editor for the *Computer Networks* (Elsevier), *Transactions on Mobile Computing and Applications* (ICST), and for the *Journal of Sensors* (Hindawi). He serves in the technical program committees of several leading conferences in wireless communications and networking, including IEEE Infocom, ACM Mobicom, and ACM Mobihoc. He was the technical co-chair of the Ad Hoc and Sensor Networks Symposium for IEEE ICC 2009. His current research interests are in modeling and optimization of multi-hop wireless networks, cross-layer design and optimization, wireless multimedia sensor and actor networks, underwater acoustic networks, and cognitive radio networks.



**Ian F. Akyildiz** is the Ken Byers Distinguished Chair Professor with the School of Electrical and Computer Engineering, Georgia Institute of Technology and Director of Broadband and Wireless Networking Laboratory. He is the Editor-in-Chief of *Computer Networks*, *Ad Hoc Networks*, and *Physical Communication Journals* (all with Elsevier). Dr. Akyildiz is an IEEE FELLOW (1995) and an ACM FELLOW (1996). He served as a National Lecturer for ACM from 1989 until 1998 and received the ACM Outstanding Distinguished Lecturer Award for

1994. Dr. Akyildiz received the 1997 IEEE Leonard G. Abraham Prize award (IEEE Communications Society) for his paper entitled "Multimedia Group Synchronization Protocols for Integrated Services Architectures," published in the *IEEE JOURNAL ON SELECTED AREAS IN COMMUNICATIONS (JSAC)* in January 1996. Dr. Akyildiz received the 2002 IEEE Harry M. Goode Memorial award (IEEE Computer Society) with the citation "for significant and pioneering contributions to advanced architectures and protocols for wireless and satellite networking." Dr. Akyildiz received the 2003 IEEE Best Tutorial Award (IEEE Communication Society) for his paper entitled "A Survey on Sensor Networks," published in *IEEE Communication Magazine*, in August 2002. Dr. Akyildiz received the 2003 ACM SIGMOBILE award for his significant contributions to mobile computing and wireless networking. His current research interests are in cognitive radio networks, sensor networks, and wireless mesh networks.